HHS Public Access

Author manuscript

Microcirculation. Author manuscript; available in PMC 2018 August 01.

Published in final edited form as:

Microcirculation. 2017 August ; 24(6): . doi:10.1111/micc.12369.

Vasoactive effect of fibronectin-derived Epiviosamine-1 and related peptides in quiescent and stress models

Mary D Frame[1,2], **Fubao Lin**[1], **Anthony M Dewar**[1], and **Richard AF Clark**[1,3]

[1]Department of Biomedical Engineering, Stony Brook University, Stony Brook, NY 11794-5281, USA

[2]Department of Physiology and Biophysics, Stony Brook University, Stony Brook, NY 11794-5281, USA

[3]Department of Dermatology, Stony Brook University, Stony Brook, NY 11794-5281, USA

Abstract

Objective—Following thermal burn injury, plasma fibronectin degrades within the interstitium; one possible product is epiviosamine-1 (EVA-1, PSHISKYILRWRPK) found within the first type III repeat of plasma fibronectin ($FNIII_1$). EVA-1 ameliorates thermal burn injury progression, and binds to and enhances platelet-derived growth factor-BB (PDGF-BB) in promoting cell metabolism, growth and survival; shorter related peptides lose these abilities. Here we study the effect of EVA-1 and shorter peptides for their vasoactivity under quiescent and stress conditions.

Materials—Using the hamster cheek pouch intravital microscopy model, five EVA-1 related peptides were applied to small arterioles via micropipette (10^{-16}–10^{-4}M) in quiescent tissue and after defined stress: nitric oxide or heat.

Results—Peak dilation occurred with nanomolar doses (longer peptides) or below (shorter peptides), blocked by propranolol (beta-adrenergic receptor antagonist). Micromolar doses of the same peptides induced only constriction, not antagonized by phentolamine (alpha-adrenergic receptor antagonist). Scrambled variants of two peptides yielded only constriction, suggesting constriction might be due peptide charge. Each stressor caused a left shift in dilation response, blocked by carazolol.

Conclusions—Thus, this important region of $FNIII_1$ contains sequences that have a gradation of biological functions dependent on the length of the peptide sequence, with increased efficacy for dilation following stressors.

Keywords

fibronectin; fibroblast; bioactive peptides; endothelial dysfunction

Corresponding author: Mary D Frame, PhD, Department of Biomedical Engineering, Physiology and Biophysics, Bioengineering G19, Stony Brook University, Stony Brook, NY 11794-5281, Phone 1-631-632-1625; Fax 1-631-632-3222; mary.frame@stonybrook.edu.

CONFLICT OF INTEREST

Richard Clark and Fubao Lin co-discovered EVA-1. Richard Clark is President and Founder of NeoMatrix Therapeutics, a biotechnology company that has acquired Orphaned Drug Designation of P12 for treatment of burns and has been engaged in preclinical studies of EVA-1.

INTRODUCTION

It has long been known that FN binds to growth factors and thereby enhances growth factor activity (17,20,32). More recently, the Clark laboratory reported that a novel peptide EVA-1, previously called P12, from the first type three repeat of plasma fibronectin, ($FNIII_1$ domain of fibronectin (FN)) has several unique biological functions: it binds PDGF-BB, enhances PDGF-BB ability to promote metabolism, proliferation, and survival of cultured adult human dermal fibroblasts, and also limits thermal burn injury progression in a rat hot comb model (18). Thermal burn injury progression is a serious clinical scenario in which damage caused by thermal burn injury becomes progressively worse over time (14), and includes oxidative damage (27). Importantly, EVA-1 is derived from fibronectin and shows a high specificity for binding PDGF-BB (18). Increased cell survival with EVA-1 was secondary to decreased apoptosis of stressed cells and was likely mediated through diminished JNK phosphorylation (18) and sustained Akt phosphorylation (35). EVA-1 represents a new class of bioactive peptides that bind to growth factors, and thereby promote the cell survival activity of growth factors. The name, epiviosamines, is derived from the Greek word *epivios*, the adjective of the verb epiviono, which means “to survive in the face of adversity”, combined with “amine” for peptide (18).

While one mechanism for EVA-1 to ameliorate thermal burn injury progression is most certainly cell survival related, other factors to consider include whether the peptide is a vasodilator acting to improve oxygenation of the thermal burn margin (zone of potential ischemia (14)). Several peptides from $FNIII_1$ have vasoactive effects at high concentrations. The Hocking group has shown that peptides from this region of FN induced either vasodilation or vasoconstriction in small arterioles, depending on the amino acid sequence (12). Peptides containing the heparin-binding domain induced vasodilation, and others caused constriction. The dosages used in that study were in the micro- to milli-molar range. Further, the Clark laboratory has recently shown that erythrocyte aggregation near a thermal burn injury is decreased by EVA-1 treatment in the nano-molar range (2). Because cell and tissue survival responses were likewise elicited by EVA-1 at a lower range (nano- to micro-molar), we tested the potential vasoactivity in this lower range. We define the vasoactive responses using the peripheral mucosal arterioles of the hamster cheek pouch *in situ* assay, as we have previously demonstrated (4). This model system addresses major receptor system(s) that may be involved in vasoactive responses to FN peptides, and facilitated use of two defined stress protocols: nitrosative stress and thermocouple controlled thermal injury.

Peptides studied here include EVA-1 (PSHISKYILRWRPK), P18 (YILRWRPK), P7 (ILRWRPK), P39 (LRWRPK) and P37 (RWRPK). These sequences were tested because they exhibit a differential biological effect for cell survival and PDGF-BB binding (Table 1), and because some peptides previously demonstrated vasoactivity (12). EVA-1 robustly binds PDGF-BB with a KD of 200nM while P7 binds with a KD of only 1μM; peptides smaller than EVA-1 do not confer cell survival activity (18). We therefore hypothesized that in healthy quiescent tissue, vasoactivity of these peptides would be sequence specific. We found that all peptide fragments induced vasoconstriction in the micromolar range, confirming findings by Hocking, et al. (12). However, at lower nano-molar dosages, peptides

induced vasodilation with a peak potency that shifted from 10^{-9}–10^{-8}M down to 10^{-11}M as the peptide shortened (Table 1). Thus, receptor-linked vasodilation to FN for these peptides are possible in healthy quiescent tissue. Further, in each stressor model, the dilation profile to EVA-1 and shorter peptides were significantly left shifted, with a peak at 10^{-13}M to 10^{-15}M.

MATERIALS AND METHODS

Intravital microscopy of the hamster cheek pouch tissue

With approval of the Stony Brook University Institutional Animal Care and Use Committee, adult male hamsters (mean±SD, 109±40 days, 116±15 g, N=185) were anesthetized (pentobarbital 70 mg/kg), tracheostomized, and the left cheek pouch tissue was prepared for observation using intravital microscopy (4,8). Animals were kept warm at 37°C. The tissue bath contained bicarbonate buffered saline that flowed over the tissue at 5 ml/min at 37°C. Following preparation, animals were rested for 30 minutes prior to data collection.

Using a modified upright Nikon microscope, the arcade-terminal arteriolar junction was observed (25× Nikon, NA 0.35), and visualized with an intensified charge-coupled device (CCD, Dage-MTI, Indianapolis, IN) camera (Figure 1). Experiments were videorecorded using a Panasonic AG7350 SVHS system (Panasonic, Tokyo, Japan), and diameters were measured off line, calibrated with a stage micrometer. The level of the microcirculation chosen for study permits testing of two classes of arterioles, terminal and arcade. Terminal arterioles provide nutrient flow to capillaries and exhibit a greater dependence on endogenous NO mediated vasodilation than do the immediately upstream arcade arterioles. (5,19) Tone was verified using topical adenosine (10^{-4}M, vasodilator) and phenylephrine (10^{-6}M, vasoconstrictor).

Experimental protocol

Drugs and peptides were administered to the arterioles using fine glass micropipettes pulled to 10–20μm diameter tips (Kopf Instruments, Tujunga, CA, USA). Each micropipette solution contained fluorescein conjugated to dextran (10^{-6}M, 4000 MW) to confirm exposure. Exposure protocols involved 60-second exposures followed by 5 minutes recovery. Complete dose response curves to individual peptides were obtained at the same microvascular site; other peptides were tested at alternate sites in the same animal. Two to four sites were tested per animal, with the criteria that the sites were at least 1000μm from each other, to insure independent responses. In protocols requiring inhibitors, the inhibitors were applied to the tissue bath exposing all blood vessels for 5 minutes prior to and during agonist application.

Drugs and peptides tested

Full-length plasma fibronectin, FN, and several peptides within the first type III repeat ($FNIII_1$) of FN were applied via micropipette. Peptides with the conserved native sequence were: EVA-1 (PSHISKYILRWRPK), P18 (YILRWRPK), P7 (ILRWRPK), P39 (LRWRPK) and P37 (RWRPK). Additionally, scrambled variants of EVA-1 (LKHSPRWISRIPYK) and P7 (WKIPRRL), and EVA-1 capped with acetylation and amidation on the amino and

carboxy-terminus, respectively, (AP12A) were tested. To test possible receptor dependence for the vasoactive responses the beta-adrenergic receptor system was stimulated with isoproterenol and inhibited with propranolol; the muscarinic receptor system was stimulated with acetylcholine and inhibited with atropine. All peptides were obtained from American Peptide, Inc. (Sunnyvale, CA) and other reagents were obtained from Sigma-Aldrich (St. Louis, MO).

Nitrosative stress model

As previously, the nitric oxide donor, SNP, was added to the tissue bath for 2 minutes (10^{-4}M) using a wash-in wash-out protocol (5, 19). This procedure induces endothelial dysfunction, confirmed by attenuated dilation to acetylcholine (10^{-4}M); also tested were adenosine (10^{-4}M), SNP (10^{-4}M), L-arginine (10^{-4}M) and phenylephrine (10^{-4}M), using micropipette delivery. Peptide vasoactive responses were tested 15 minutes to 3 hours following nitrosative stress, and only four exposures per site following stress (5).

Microcautery induced thermal stress model

Using a microcautery system (JorVet Equip, Inc) that was temperature and time controlled by a thermocouple, heat was applied for 20s at a temperature of 50 °C. The microcautery tip was a platinum (Pt) wire, 300 μm in diameter. The estimated temperature gradient away from the 50 °C Pt wire tip dissipates over a short distance, with an estimated 37 °C at 500 μm from the rim edge; this is based on the parameters well described by Moritz (11,22,23). The temperature response of this system was determined in a stationary pool of water, using a fine temperature probe (Fisher Scientific); within 2–3 seconds, the independent temperature probe reached the desired temperature, and maintained that temperature (+/−0.5 °C) for the duration of a 20 s exposure, with 37 °C being measured approximately 600–800 μm from the heat source (data not shown). After waiting 15 min (5), vasoactive responses were mapped out to 1000 μm from the rim of the heated area (see Figure 1B), using the same agents and dosages as noted for the *Nitrosative stress model*. Responses within 500 μm of the heat rim are reported; response further than 500 μm from the heat rim are not different from control responses, and are not reported here. Likewise, higher temperatures and longer exposures resulted in endothelial dysfunction extending further than 500 μm from the heat rim, as expected (data not shown).

Statistics

Diameter change was calculated as the fractional change from baseline: [(baseline-peak)/baseline]. Comparisons were made using analysis of variance for repeated measures for the concentration response relationships, and using unpaired t-test for single dose comparisons between treatments. All experimental design used a β-probability function of 0.6, *a prior*, and a statistical significance, α-probability function of 0.05, *post hoc* (31).

RESULTS

Baseline diameters were 16±7.7μm (mean ± SD) for the larger arcade arterioles (n= 373 arterioles in N=185 animals), and 6.9±2.3μm (n=392) for the terminal arterioles. Representative images are shown in Figure 1. Adenosine (10^{-4} M) induced a significant

dilation in the arcade arterioles (0.54±0.35, fractional change from baseline, mean ± SD) and in the terminal arterioles (0.60±0.43). Phenylephrine (10^{-6}M) induced a significant constriction in the arcades (−0.53±0.18) and terminal arterioles (−0.48±0.16).

Arteriole responses to five FN peptides and intact plasma FN are shown in Figure 2. Intact plasma FN induced only vasodilation while peptides tended to induce dilation at lower doses and constriction at higher doses. EVA-1 (P12), P18 and P7 induced significant peak dilations in the nano-molar range in both classes of arterioles. The shorter peptide, P37, showed some dilation in the sub-nano-molar range in arcade arterioles. In the terminal arterioles, peak dilation was shifted to the left at 10–11M, while all peptides showed a vasodilation response at these low doses. Thus, the vasoactivity pattern appeared peptide specific with clear differences in response by the two classes of arterioles.

All of these peptides will carry a net positive charge at pH 7.4, as suggested by the pK values of the composite amino acids. To test whether constriction at high doses was due to a non-specific charge effect, we applied scrambled peptides, P12s and P7s. In both vessel types, scrambled peptides induced constriction, but not vasodilation (Figure 3). Furthermore, when EVA-1 was capped at the amino- and carboxy- ends by acetylation and amidation, respectively, dilation was eliminated and only constriction was evident at the higher doses. Thus, we presume that the constriction induced by these peptide fragments is due to a non-specific charge effect; this was further supported by more specific testing, discussed in the next few paragraphs.

Several receptor systems are linked to vasodilation (and vasoconstriction) in the hamster cheek pouch, including adrenergic and muscarinic receptors. These receptor systems were investigated (Figure 4). Alpha-adrenergic blockade (Figure 4A) was without effect; supporting our notion that constriction is a non-specific electrostatic charge effect. Phentolamine activity was validated by showing that the vasoconstriction induced by phenylephrine (10^{-5}M) (arcades −0.52±0.18; terminal −0.48±0.16) was abrogated by phentolamine (arcades −0.10±0.04; terminal −0.01±0.03) (mean ± SD, n=23 sites).

Beta-adrenergic blockade (Figure 4B) with propranolol (10^{-6}M) prevented vasodilation to peptides EVA-1 (P12), P18, P7 and P37 (P39 was not tested). Propranolol also significantly diminished dilation to full length FN, with significant residual dilation at only 10^{-6}M FN. Higher concentrations of FN were not possible to achieve due to ‘gelling’ of the solution. Activity of propranolol was tested by showing that isoproterenol (10^{-7}M) induced vasodilation (arcades 0.41±0.3, fractional change from baseline, mean ± SD; terminal 0.43±0.34) was eliminated in the presence of propranolol (arcades 0.00±0.11; terminal 0.01±0.00) (mean ± SD, n=23 sites).

Combined alpha- and beta-adrenergic blockade eliminated only the vasodilation with the peptides and not FN (Figure 4C). Lastly, scrambled EVA-1 (P12s) or P7s vasoconstriction were unaffected by alpha, beta or combined alpha/beta adrenergic blockade (not shown, n=5–7 sites per combination).

We next tested the muscarinic receptor system. Atropine (10^{-7} M), a muscarinic receptor inhibitor, had no effect on any EVA-1, P7 or FN vasoactivity (Figure 5). Atropine activity

was tested by showing that acetylcholine (10^{-4}M) induced vasodilation (arcades 0.50±0.36; terminal 0.49±0.28) was eliminated in the presence of atropine (arcades 0.03±0.15; terminal 0.03±0.10) (mean ± SD, n=26 sites). Together our results are consistent with the posit that vasodilation activity of these peptides requires beta-adrenergic receptor linked activity, while vasoconstriction more likely results from an electrostatic charge effect.

With recent evidence that in thermal burn injury EVA-1 treatment is both protective (18) and results in reduction of RBC aggregates near the thermal injury (2), we tested whether the dose response to EVA-1 was altered by stress, using 2 stress protocols: nitrosative stress and thermal stress. Endothelial dysfunction was confirmed in both the nitrosative stress model (2 minutes tissue wide exposure to an NO-donor), and the thermal stress model (50 °C, 20s, 300 μm Pt tip) (Figure 6). The hallmark response indicating endothelial dysfunction is diminished dilation to acetylcholine. Additionally, as previously with endothelial dysfunction, there is an uncovered dilation to micropipette applied L-arginine (5,19). Thus, we confirmed endothelial dysfunction in each stress model.

We further tested dilation acting through purinergic receptors on the vascular smooth muscle cells (adenosine) and smooth muscle dilation directly mediated by a nitric oxide donor (SNP). Dilation to adenosine is compromised in both models, suggestive of a wide-spread stress, and not solely endothelial dysfunction. Dilation to nitroprusside is not compromised for either model, indicating that the smooth muscle cells themselves are capable of dilating. These findings are likewise consistent with our prior studies of nitrosative stress (5,7,19,25). Constriction to phenylephrine was unaffected in either stress model. Figure 6 shows data from terminal arterioles; arcade arteriole responses exhibit a similar trend (data not shown). Thus, in each model of stress, endothelial dysfunction is apparent, and the altered vasoactive response state is equivalent.

Nitrosative stress caused a left shift in the concentration response to EVA-1, amino- and carboxyl-terminal capped EVA-1 (Ap12A), P7 and P37 (Figure 7). [For ease of comparison, the corresponding control data from prior figures are re-drawn in Figure 7.] Interestingly, while Ap12A showed minimal vasodilation activity in quiescent tissue (Figure 3), it showed robust low-dose vasodilation activity following nitrosative stress. For P37, the left shift was 2-orders of magnitude greater than for the others, peaking at 10^{-15}M. In quiescent tissue, we demonstrated that propranolol blocked vasodilation to these peptides (Figure 4). Propranolol is a broadly acting beta-adrenergic antagonist. Due to the low dosages at which vasodilation was seen, we now tested a beta-adrenergic inverse agonist, carazolol (10^{-9}M, alone not significantly vasoactive, −0.09+0.1). We confirmed that dilation to isoproterenol (10^{-6}M, terminal arterioles, 0.32+0.26, mean+sem) was eliminated by carazolol (10^{-9}M, −0.50+0.15, significant constriction). Choosing the peak dilation range of the peptides with stress (10^{-13}M), in the presence of carazolol (10^{-9}M), EVA-1 had no effect (−0.01+0.006), and capped EVA-1 (Ap12A) induced constriction (−0.14+0.04). The arcade arterioles showed a similar trend, although diminished in magnitude (data not shown). Thus, the low dose dilation uncovered by nitrosative stress was beta-adrenergic receptor linked.

This effect of stress was further tested using the thermal stress model (Figure 8). With thermal stress, dilation at 10^{-8}M was eliminated in terminal arterioles, and reversed to

constriction in the arcade arterioles. However, a significant vasodilation to sub-nanomolar EVA-1 was observed in both arteriolar types after thermal stress, as with nitrosative stress.

DISCUSSION

In healthy quiescent tissue, five overlapping peptides from the first type three repeat of plasma fibronectin, $FNIII_1$ each individually induce vasodilation in small arterioles at nano-molar doses and constriction at micro-molar doses. Constriction appears to be non-specific and we speculate that is it due to excess cationic charge carried by the peptides. Dilation appears to be specifically linked to beta-adrenergic receptor related events. Using two stress models, in which endothelial dysfunction is apparent, the concentration response for vasodilation to these peptides is shifted to the left, well into the nano- to pico-molar range; this also appears to be related to beta-adrenergic receptor activity.

Our key finding relates vasodilation to the total picture of biological activity of these important peptides. The biological activity of these peptides appears to shift with decreasing dosage, from enabling survival, to growth factor binding, to highly efficacious vasodilation as the sequence EVA-1 loses amino acids from the amine terminus, which is further enhanced in a stress model (Table 1). Importantly, fragmentation of FN within the interstitial compartment produces YILRWRPK (P18), and human neutrophil elastase digestion of EVA-1 produces RWRPK (P37) and LRWRPK (P39) as end-products (Lin, Rieger and Clark, unpublished observations). Thus, the peptides we tested can form endogenously upon damage to the microcirculatory vessels that would permit plasma fibronectin release to the interstitium.

These plasma fibronectin peptides have multiple biological effects related to their sequence and length (Table 1). EVA-1 (previously called P12), the longest, confers survival activity at 10^{-7}M, binds PDGF-BB at 10^{-8}–10^{-7}M and we now show, vasodilates the mucocutaneous microvasculature at 10^{-9}–10^{-8} M. Shorter peptides loose survival activity. P7 binds PDGF-BB with lowered affinity (micromolar range), but remains a vasodilator at 10^{-9}–10^{-8}M. The shortest peptide tested, P37 (RWRPK), induced vasodilation with very high affinity in the terminal arterioles (10^{-11}M) or arcade arterioles (10^{-10}M). All three (EVA-1, P7 and P37) display pico- to femto-molar dose vasodilation after stress, with the smallest peptide P37 being the most efficacious. Thus the gradation in vasoactive response is related to the peptide length in both quiescent and stressed tissue.

Fibronectin (FN) has been shown to play a vital role in wound healing (30) and is deficient in the wounds and blood of patients with burns (16). Recently the Clark laboratory has demonstrated that EVA-1 (previously called P12) promotes adult human dermal fibroblast survival when cultured under stress conditions such as ROS or ER stress and limits burn injury progression in a rat hot comb model (18). Since others have suggested that ROS stress from ischemia-reperfusion may be part of the pathogenesis of burn injury progression (15,27), it is possible that EVA-1 might limit burn injury progression through its ability to limit interstitial cell injury from ROS (18) or through its ability to vasodilate the cutaneous microvasculature as suggested by the data in this study, or by both mechanisms.

The peptides we tested are contained within the larger FN fragment known as anastellin, a potent anti-angiogenic peptide that has not been reported to have vasoactive activity (28). The study by Hocking, et al., (12) shows that peptides from FN containing the heparin binding site to be vasodilatory in the micromolar range and a sequence closely related to those we tested to be vasoconstrictory. The mechanism responsible for vasoactivity was not tested. In endothelial cell culture, the McKeown-Longo group has demonstrated that anastellin inhibits the ras/ERK pathway (1) and activates p38 MAPK in an integrin (β_1) independent manner (34). Smaller fragments of anastellin were not tested. Thus, little was known about the vasoactivity mechanism of these $FNIII_1$ peptides.

We show the interesting and novel link between vasodilation induced by exposure to these small peptides and beta-adrenergic receptor linked activity. Others have shown that intraluminal endothelial cell binding peptides from plasma fibronectin, in particular the RGD sequence, prevents flow mediated dilation that involves the β3-integrin subunit (24), and lower plasma fibronectin concentration in whole blood is associated with a diminished reactive hyperemic vasodilation in pregnant and pre-eclamptic humans (33). Abluminal fibronectin, again the RGD sequence, has been linked to vascular smooth muscle constriction that involves the $\alpha_5\beta_1$ integrin receptor (13,21,24). Thus, fibronectin-induced vasoconstriction has been linked to integrin binding, while here we demonstrate that fibronectin and fibronectin peptide vasodilation is related to beta-adrenergic receptor activity.

Secondarily, we reinforce the physiological differences between the arcade arterioles, which feed terminal arteriolar networks (hence are ‘conduit’ arterioles), and the terminal arteriolar networks, which feed only the nutrient exchange capillary vessels. The responses of the terminal and arcade arterioles in this tissue, and in others, differ in response to a range of vasoactive agents (4,7,8). For many agonists, the differences in responsivity seen with the two classes of arterioles appears to be due to a synergy between phosphodiesterase (PDE) 3 and 4 (i.e., cGMP vs. cAMP) to maintain tone in the terminal arterioles, and predominantly cAMP in the arcade arterioles (5,19). Whether this is the reason for the change in affinity for FN peptides to cause vasodilation here is beyond the scope of the study. We clearly show that the terminal arterioles are more responsive to these peptides than the arcade arterioles.

Our primary finding is that the $FNIII_1$ peptide EVA-1 displayed nuanced vasoactive behavior. Of key interest is the specific vasodilation in the nanomolar range and lower. In addition, our data provides a clear example of differential biological function obtained by shortening peptides within $FNIII_1$, i.e. transition from endothelial cell and angiogenesis inhibition (anastellin, a 76 amino acid fragment of $FNIII_1$), to endothelial cell survival and angiogenesis (a 25mer fragment of anastellin, McTigue and Clark, unpublished observations), to fibroblast survival and growth factor binding (14mer EVA-1), and to vasoactivity (EVA-1 and shorter peptides).

Acknowledgments

None

Grant support: NIH HL55492 (MF); AHA 0655908T (MF); Armed Forces Institute of Regenerative Medicine W81XWH-08-2-0034 (RAFC).

Abbreviations

Akt	Protein kinase B
erk	estracellular-signal-regulated kinases
EVA-1	epiviosamine-1, PSHISKYILRWRPK
FAK	focal adhesion kinase
FN	plasma fibronectin
FNIII1	first type three repeat of plasma fibronectin
JNK	c-Jun N-terminal kinases
KD	dissociation constant
MAPK	mitogen activated protein kinase
NO	nitric oxide
P7	ILRWRPK
P7s	WKIPRRL
P12	EVA-1
P12s	LKHSPRWISRIPYK
P18	YILRWRPK
P37	RWRPK
P39	LRWRPK
PDGF-BB	platelet derived growth factor BB
ras	small GTPase
ROS	reactive oxygen species

References

1. Ambesi A, McKeown-Longo PJ. Anastellin, the angiostatic fibronectin peptide, is a selective inhibitor of lysophospholipid signaling. Mol Cancer Res. 2009; 7:255–65. [PubMed: 19208746]
2. Asif B, Abdul R, Fenner J, Lin F, Hirth DA, Hassani J, McClain SA, Singer AJ, Tonnesen MG, Clark RAF. Blood vessel plugging in periburn tissue is secondary to erythrocyte aggregation and mitigated by a fibronectin-derived peptide that limits burn injury progression. Wd Rep Regen. 2016; 24:501–513.
3. Braverman IM. The Cutaneous Microcirculation: ultrastructure and microanatomical organization (Review). Microcirculation. 1997; 4:329–40. [PubMed: 9329009]

4. Dewar A, Clark RAF, Singer AJ, Frame MD. Curcumin mediates both dilation and constriction of peripheral arterioles via adrenergic receptors. J Invest Dermatol. 2011; 131:1754–1760. [PubMed: 21525885]
5. Frame MD, Mabanta L. Remote microvascular preconditioning alters specific vasoactive responses. Microcirculation. 2007; 14:739–751. [PubMed: 17885998]
6. Frame MD, Rivers RJ, Altland O, Cameron S. Mechanisms initiating integrin stimulated flow recruitment in arteriolar networks. J Appl Physiol. 2007; 102:2279–87. [PubMed: 17379749]
7. Frame MD, Fox R, Kim D, Mohan A, Berk BC. Diminished arteriolar responses in nitrate tolerance involve ROS and angiotensin II. Am J Physiol Heart Circ Physiol. 2002; 282:H2377–H2385. [PubMed: 12003849]
8. Georgi MK, Dewar AM, Frame MD. Downstream Exposure to Growth Factors Causes Elevated Velocity and Dilation in Arteriolar Networks. J Vas Res. 2011; 48:11–22.
9. Gyorfi A, Fazekas A, Rosivall L. Neurogenic inflammation and the oral mucosa (review). J Clin Periodontol. 1992; 19:731–6. [PubMed: 1280655]
10. Hardman, JG., Limbird, LE., editors. Goodman and Gilman's The Pharmacological Basis of Therapeutics. 9th. McGraw-Hill; New York: 2001. p. 199-248.
11. Henriques FC Jr, Moritz AR. Studies of Thermal Injury. I. The Conduction of Heat to and through Skin and the Temperatures Attained Therein. A Theoretical and an Experimental Investigation. Am J Pathology. Aug.1947 :531–549.
12. Hocking DC, Titus PA, Sumagin R, Sarelius IH. Extracellular matrix fibronectin mechanically couples skeletal muscle contraction with local vasodilation. Circ Res. 2008; 102:372–379. [PubMed: 18032733]
13. Hong Z, Sun Z, Li Z, Mesquitta WT, Trzeciakowski JP, Meininger GA. Coordination of fibronectin adhesion with contraction and relaxation in microvascular smooth muscle. Cardiovasc Res. 2012; 96:73–80. [PubMed: 22802110]
14. Jackson DM. The diagnosis of the depth of burning. The British Journal of Surgery. 1953; 40(164): 588–96. [PubMed: 13059343]
15. Jaskille AD, Jeng JC, Sokolich JC, Lunsford P, Jordan MH. Repetitive ischemia-reperfusion injury: a plausible mechanism for documented clinical burn-depth progression after thermal injury. J Burn Care Res. 2007; 28:13–20. [PubMed: 17211195]
16. Lanser ME, Saba TM, Scovill WA. Opsonic glycoprotein (plasma fibronectin) levels after burn injury. Relationship to extent of burn and development of sepsis. Ann Surg. 1980; 192:776–82. [PubMed: 7447531]
17. Lin F, Ren XD, Pan Z, Macri L, Zong WX, Tonnesen MG, Rafailovich M, Bar-Sagi D, Clark RA. Fibronectin growth factor-binding domains are required for fibroblast survival. J Invest Dermatol. 2011; 131:84–98. [PubMed: 20811396]
18. Lin F, Zhu J, Tonnesen MG, Taira BR, McClain SA, Singer AJ, Clark RA. Novel fibronectin peptides bind PDGF-BB and enhance cell and tissue survival under stress. J Invest Dermatol. 2014; 134:1119–1127. [PubMed: 24126844]
19. Mabanta L, Valane P, Borne J, Frame MD. Initiation of remote microvascular preconditioning requires KATP channel activity. Am J Physiol Heart Circ Physiol. 2006; 290:H264–H271. [PubMed: 16126818]
20. Martino MM, Hubbell JA. The 12th–14th type III repeats of fibronectin function as a highly promiscuous growth factor-binding domain. FASEB Journal. 2010; 24:4711–4721. [PubMed: 20671107]
21. Mogford JE, Davis GE, Meininger GA. RGDN peptide interaction with endothelial alpha5beta1 integrin causes sustained endothelin-dependent vasoconstriction of rat skeletal muscle arterioles. J Clin Invest. 1997; 100:1647–53. [PubMed: 9294134]
22. Moritz AR, Henriques FC Jr. Studies of Thermal Injury. II. The Relative Importance of Time and Surface Temperature in the Causation of Cutaneous Burns. Am J Pathology. Sep.1947 :695–720.
23. Moritz AR. Studies of Thermal Injury. III. The Pathology and Pathogenesis of Cutaneous Burns. An Experimental Study. Am J Pathology. Nov.1947 :915–941.
24. Muller JM, Chilian WM, Davis MJ. Integrin signaling transduces shear stress–dependent vasodilation of coronary arterioles. Circ Res. 1997; 80:320–6. [PubMed: 9048651]

25. Mustafa SS, Rivers RJ, Frame MDS. Microcirculatory basis for non-uniform flow delivery with intravenous nitroprusside. Anesthesiology. 1999; 91(3):723–731. [PubMed: 10485784]
26. Oaklander AL, Siegel SM. Cutaneous innervation: form and function (review). J Am Acad Dermatol. 2005; 53:1027–37. [PubMed: 16310064]
27. Parihar A, Parihar MS, Milner S, Bhat S. Oxidative stress and anti-oxidative mobilization in burn injury. Burns. 2008; 34:6–17. [PubMed: 17905515]
28. Ruoslahti, E., Yi, M. Methods of inhibiting tumor growth and angiogenesis with anastellin. US. 20030091556 A1. Dec 3. 2003 filing date
29. Scardina GA, Ruggieri A, Messina P. Oral microcirculation observed in vivo by videocapillaroscopy: a review. J Oral Sci. 2009; 51:1–10. [PubMed: 19325194]
30. Singer AJ, Clark RA. Cutaneous wound healing. N Engl J Med. 1999; 341(10):738–46. [PubMed: 10471461]
31. Snedecor, GW., Cochran, WG. Statistical Methods. The Iowa State University Press; Ames: 1974. p. 593
32. Wijelath ES, Rahman S, Namekata M, Murray J, Nishimura T, Mostafavi-Pour Z, Patel Y, Suda Y, Humphries MJ, Sobel M. Heparin-II domain of fibronectin is a vascular endothelial growth factor-binding domain: enhancement of VEGF biological activity by a singular growth factor/matrix protein synergism. Circ Res. 2006; 99:853–860. [PubMed: 17008606]
33. Yoshida A, Nakao S, Kobayashi M, Kobayashi H. Flow-mediated vasodilation and plasma fibronectin levels in preeclampsia. Hypertension. 2000; 36:400–4. [PubMed: 10988272]
34. You R, Klein RM, Zheng M, McKeown-Longo PJ. Regulation of p38 MAP kinase by anastellin is independent of anastellin's effect on matrixfibronectin. Matrix Biol. 2009; 28:101–9. [PubMed: 19379667]
35. Zhu J, Lin F, Brown D, Clark RA. A fibronectin peptide redirects PDGF-BB/PDGFR complexes to a macropinocytosis-like pathway and augments PDGF-BB survival signals. J Invest Dermatol. 2014; 134:921–929. [PubMed: 24304816]

PERSPECTIVES

Thermal burn injury progression is categorized as a clinical condition with a, ‘serious unmet need’, in which treatment options are little other than palliative measures. The peptides we have tested, EVA-1 in particular, show a striking potential to satisfy this unmet need even when administered up to 12 hours post-burn (Lin and Clark, unpublished results). Limiting burn injury by epiviosamine-1 can speed healing thereby reduce need for surgery, patient suffering, and hospital cost in the short term; and mitigate scarring (2) thereby improving quality of life long term. The present manuscript contributes understanding of the dose and, ‘state dependent’, mechanism(s) of action of EVA-1 and its analogue peptides in the quiescent vs stress states.

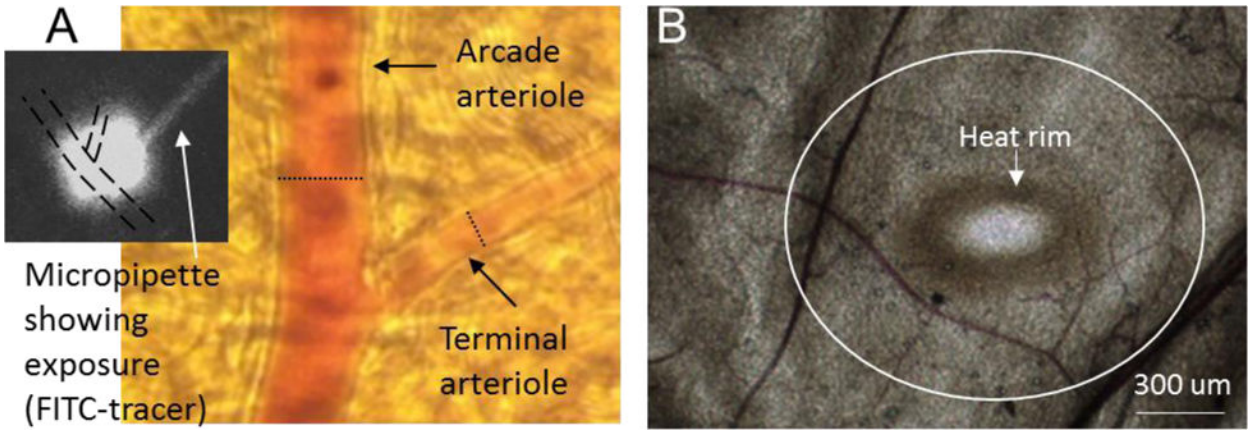

Figure 1.

(A) Micrograph taken at the microscope eyepiece using an iPhone 3. The dotted scale bar shows the diameter of a maximally dilated arcade arteriole at that location (21.3 μm) and of a maximally dilated terminal arteriole (8.7 μm). The black and white inset is digitized from the video image showing the micropipette containing FITC-dextran, and the exposure 'cloud' that saturates both arterioles with one exposure. Diameters were measured at the regions exposed to micropipette contents. (B) Micrograph taken with a Retiga color camera to illustrate the tissue following thermal stress. The heat rim is readily apparent following 20s exposure to 50 °C; no rim is seen if the Pt wire is gently laid on the overlying connective tissue without heat. The white circle outlined the approximate dimensions of 500 um from the heat rim; data was taken within 1000 um of the heat rim. The estimated temperature gradient is given in the Discussion.

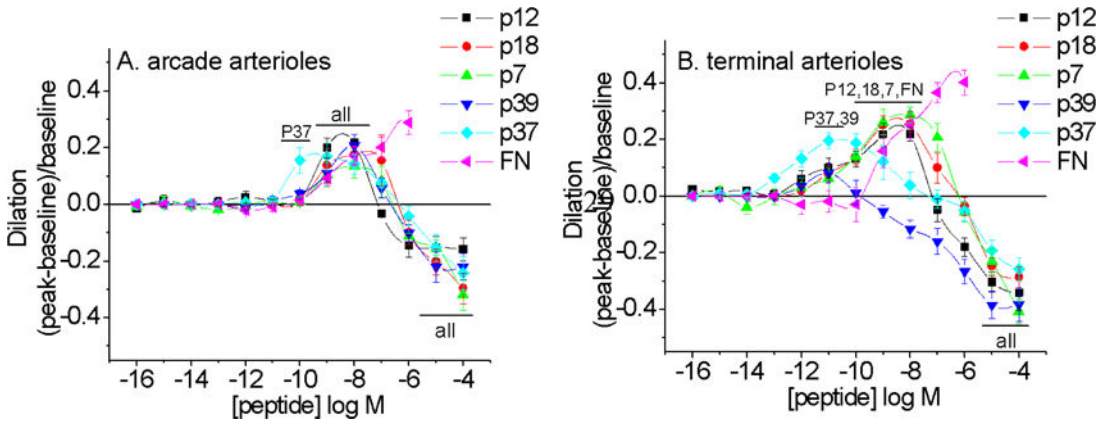

Figure 2.

Vasoactive responses to $FNIII_1$-derived peptides and full length plasma fibronectin (FN) for arcade arterioles (A) and terminal arterioles (B). Sequences are given in the text and EVA-1 is denoted P12 in figure. Some, but not all, smaller peptides were more efficacious vasodilators, but all peptides stimulated vasoconstriction at micromolar doses. Not all significant responses are noted. N=5–8 per peptide. All peptides exhibit vasoactive responses significantly different from baseline diameter (bars labeled “all”); bars labeled with peptides elicited significant dilation responses. Significance level $p<0.05$.

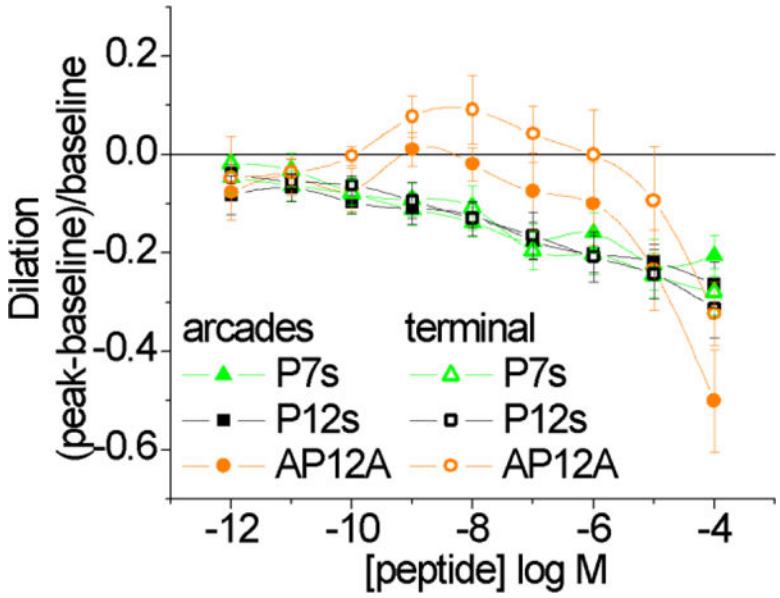

Figure 3.

Arcade and terminal arteriole vasoactive responses to scrambled EVA-1 (P12s) and scrambled P7 (P7s), and to acetylated and amidated EVA-1 (AP12A). Scrambled and AP12A peptides induced significant constriction of arcades from 10^{-10} – 10^{-4}M and 10^{-4}M, respectively. Dilation of the terminal arterioles to AP12A at 10^{-8}M has a p-value = 0.13, and therefore is not significant. Significance level $p<0.05$.

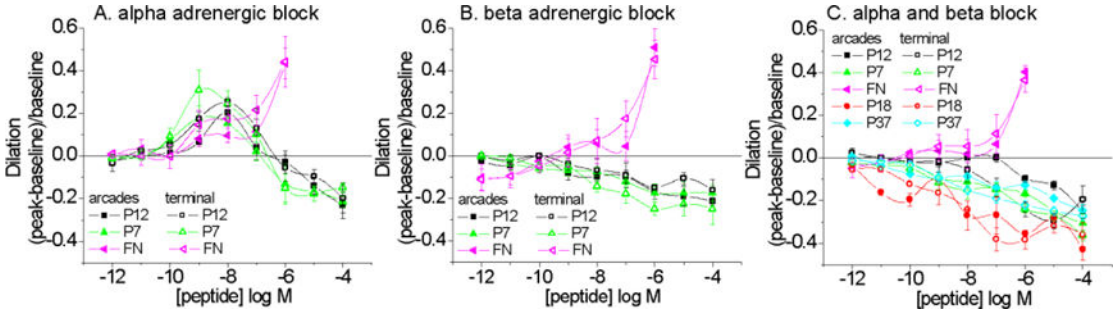

Figure 4.

Arcade and terminal arteriole vasoactive responses to peptides during alpha adrenergic blockade with phentolamine (A. 10^{-5}M), beta adrenergic blockade with propranolol (B. 10^{-6}M), or both (C). EVA-1 is denoted as P12. With alpha adrenergic block, dilation results remained significant. Significance level $p<0.05$.

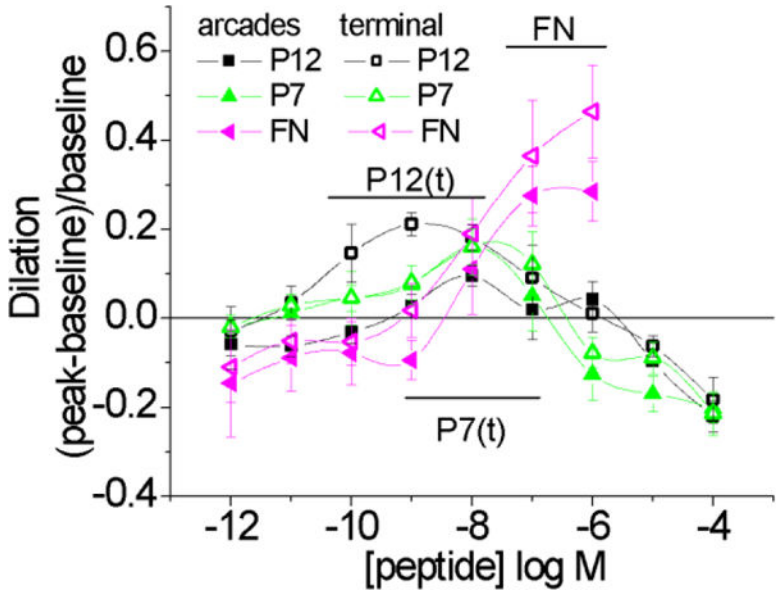

Figure 5.

Vasoactive responses to peptides during muscarinic blockade with atropine (10–6M) for arcade arterioles (arcades) and terminal arterioles (terminal). Dilation to fibronectin remained significant for both classes of arterioles (bar marked FN). Dilation to EVA-1 (P12) and P7 remained significant for the terminal arterioles (bars marked P12(t) and P7(t)). For the arcade arterioles, dilation to EVA-1 (P12) and P7 remained significant at 10^{-8}M only. Significance level $p<0.05$.

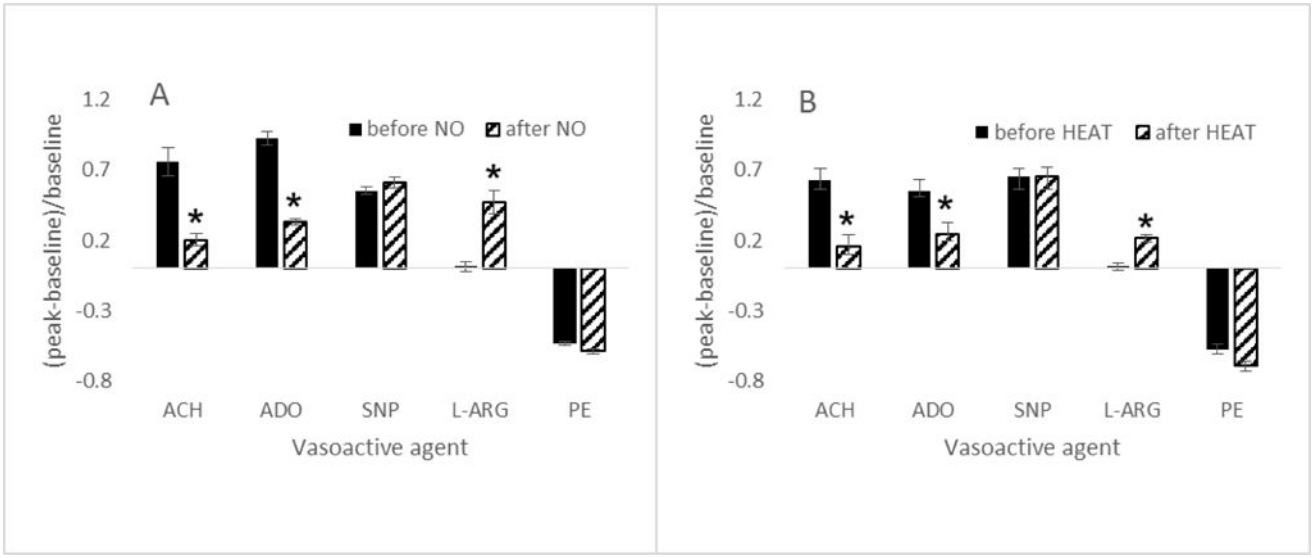

Figure 6.

Vasoactive responses of terminal arterioles to acetylcholine (ACH, 10-4M), adenosine (ADO, 10-4M), nitroprusside (SNP, 10-4M), L-arginine (L-ARG, 10-4M) and phenylephrine (PE, 10-4M) before and after stress induced by (A) 2 minutes exposure to tissue wide NO (nitric oxide donor, SNP, 10-4M, n=35) or (B) 20 seconds exposure to 50 dC heat delivered via a 300 um Pt wire (thermocouple controlled, n=27). Responses in (B) were obtained within 500 um of the Pt wire. *differs from before; significance level $p<0.05$.

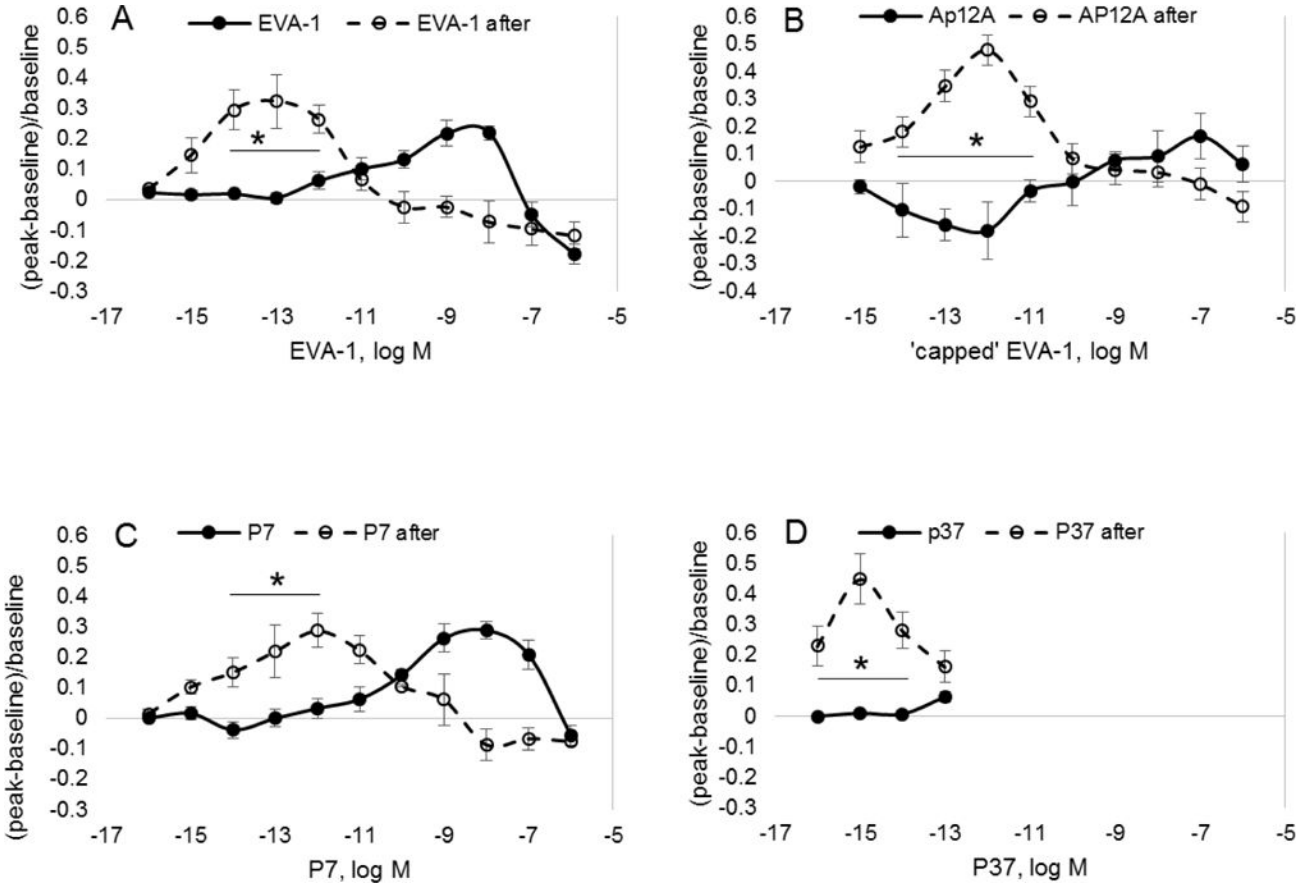

Figure 7.

Shown are vasoactive responses to EVA-1, capped EVA-1 (AP12A), P7 and P37 before (solid circles) and after (open circles) tissue bath exposure to the nitric oxide donor, SNP, for 2 minutes (10-4M). In each case, nitrosative stress induced a significant left shift in the concentration response curve. *differs from baseline state; significance level $p<0.05$.

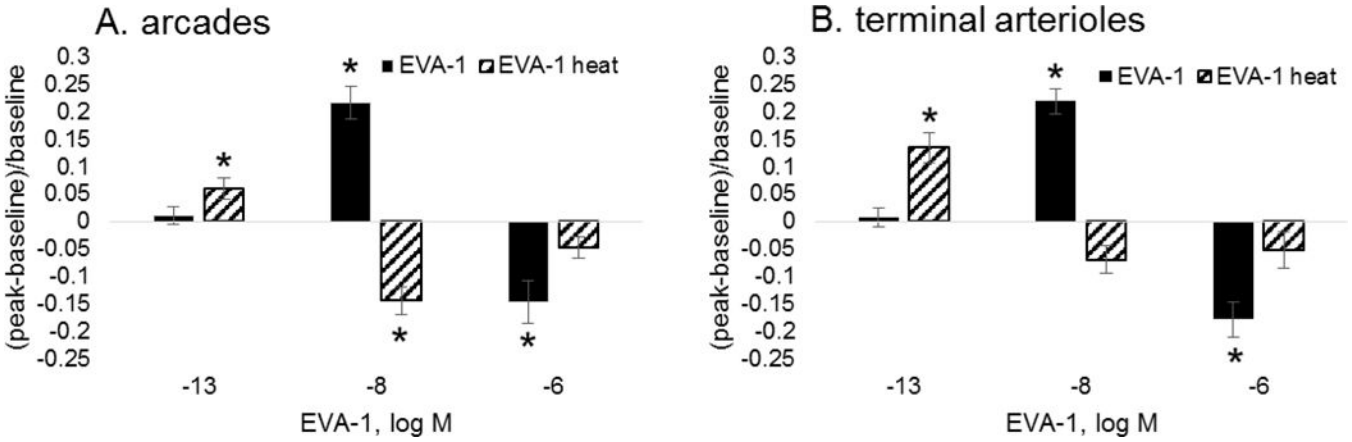

Figure 8.

Shown are vasoactive responses for arcade (A) and terminal arterioles (B) during exposure to EVA-1 before (solid) and after (hatched) thermal burn injury stress (20s, 50 dC). All responses were obtained within 500 μm of the burn rim. *differs from baseline diameter; significance level $p<0.05$.

Table 1

Summary of the biological effects of the peptide fragments contained within the 1st type III repeat of plasma fibronectin, ($FNIII_1$).

Peptide	*Peptide sequence*	*Survival activity*[a]	*FN/PDGF-BB binding inhibition*[b]	*Control*[c]		*Stress*[c]	
				Dose (%) Max dilation		*Dose (%) Max dilation*	
EVA-1	PSHISKYILRWRPK	Yes	95.5%	10^{-9}M	22%	10^{-13}M	32%
P18	YILRWRPK	No	26%	10^{-8}M	26%	–	–
P7	ILRWRPK	No	0.1%	10^{-8}M	28%	10^{-12}M	29%
P39	LRWRPK	No	0.0%	10^{-11}M	8%	–	–
P37	RWRPK	No	0.0%	10^{-11}M	19%	10^{-15}M	45%

[a](ref #17, Lin, et al., 2011);

[b](Ref #18, Lin, et al., 2014; Ref #35, Zhu, et al., 2014);

[c]present study, terminal arterioles.